

# Photocatalytic degradation of a model textile dye using Carbon-doped titanium dioxide and visible light

Giuseppe Cinelli<sup>a§</sup>, Francesca Cuomo<sup>a§</sup>, Luigi Ambrosone<sup>b</sup>, Matilde Colella<sup>c</sup>, Andrea Ceglie<sup>a</sup>,  
Francesco Venditti<sup>a\*</sup>, Francesco Lopez<sup>a\*</sup>

<sup>a</sup>Department of Agricultural, Environmental and Food Sciences (DiAAA) and Center for Colloid and Surface Science (CSGI), Università degli Studi del Molise, Via De Sanctis, I-86100 Campobasso, Italy.

<sup>b</sup>Department of Medicine and Health Sciences “Vincenzo Tiberio”, Università degli Studi del Molise, Via De Sanctis, I-86100 Campobasso, Italy.

<sup>c</sup>Dipartimento di Bioscienze, Biotecnologie e Biofarmaceutica, Università degli Studi di Bari “Aldo Moro”, Bari, Italy.

§ These two authors contributed equally to this work.

\*Corresponding authors:

Francesco Lopez, Department of Agricultural, Environmental and Food Sciences and Center for Colloid and Surface Science (CSGI), Università degli Studi del Molise, via De Sanctis, I-86100 Campobasso, Italy. Phone: +39 0874404632; fax: +39 0874404652; mail: [lopez@unimol.it](mailto:lopez@unimol.it).

Francesco Venditti, Department of Agricultural, Environmental and Food Sciences and Center for Colloid and Surface Science (CSGI), Università degli Studi del Molise, via De Sanctis, I-86100 Campobasso, Italy. Phone: +39 0874404633; fax: +39 0874404652; mail: [francesco.venditti@gmail.com](mailto:francesco.venditti@gmail.com).

34 **Abstract**

35 Rhodamine B (RhB), a dye widely used in the textile manufacturing, contributes with other dyes to  
36 harm the environment. Here, with the final goal to provide new tools for the removal of dyes from  
37 water, a visible light activated carbon-doped titanium dioxide was used to investigate on the  
38 decolourization and the photocatalytic degradation of RhB dye from water solutions. The  
39 photodegradation activity was tested varying the initial concentration of RhB and the amount of  
40 carbon-doped titanium dioxide, taking into account the ratio between the amount of catalyst and the  
41 amount of RhB ( $\text{TiO}_2/\text{RhB}$ ), thus obtaining a parameter that allows the method to be scaled up  
42 without losing its effectiveness. Values of  $k_2$  and  $t_{0.5}$  were obtained by fitting kinetics data to a  
43 second-order kinetic adsorption model. The important role played by doped  $\text{TiO}_2$  particles is  
44 demonstrated by the highly efficient color removal obtained during the visible light-induced  
45 photocatalysis. The presence of different degradation intermediates was demonstrated by means of  
46 UV-Visible Absorption and Fluorescence spectroscopy. Such results underline that the whole  
47 photodegradation process does not end with the decolourization occurrence.

48

49 **Keywords:** Water treatment,  $\text{TiO}_2$ , Photocatalysis, Dye, Kinetics, Fluorescence.

50

## 51 **1. Introduction**

52 Dye pollutants produced from the textile manufacturing are becoming a serious source of  
53 environmental contamination [1, 2]. It is estimated that thousands of different dyes and pigments  
54 are used industrially and an enormous number of synthetic dyes are yearly produced worldwide.  
55 Textile factories are second only to agriculture in the amount of pollution they create and the large  
56 amounts of water they use. Pollutants released by the global textile industry are continuously doing  
57 incredible harm to the environment, polluting lands and making them useless and unproductive [3].

58 Dyes are substances widely used in textile, as well as in pharmaceutical, food, plastics, paper  
59 manufacturing [4-8]. The chromophores, responsible for the specific dye color, are classified  
60 according to their chemical structure and their application field. The chromophore-containing  
61 centers are based on various functional groups, among these the main are azo, anthraquinone,  
62 methine, nitro, arylmethane, carbonyl groups. Donating substituents able to generate color  
63 amplification of the chromophores are denominated auxochromes (amine, carboxyl, sulfonate and  
64 hydroxyl).

65 Among these molecules Rhodamine B (RhB) is a fluorescent cationic dye widely used in textile  
66 dyeing because of its more rigid structure than other organic dyes, and is also a well-known  
67 fluorescent water tracer [9]. Due to its cationic structure, it can be used for anionic fabrics that  
68 contain negative charges such as polyester fibers. RhB results harmful to human and animals: it  
69 causes irritation of the skin, eyes and respiratory tract. Also, Rhodamine dyes are highly toxic to  
70 reproductive and nervous systems and it has been proven that drinking water contaminated with  
71 Rhodamine could lead to subcutaneous tissue borne sarcoma [10].

72 Worldwide regulations for industrial wastewater require significant elimination of the dyestuff  
73 amount from the effluent [11]. Nevertheless, it has been evaluated that a considerable part of the  
74 dyestuff is still being released to the ecosystem. Several approaches have been developed for the  
75 effluent treatment but none of them is still sufficiently effective and a combination approach seems  
76 to be so far the most efficient.

77 Generally, dyestuff is faced with chemical and physical methods, such as adsorption and bio-  
78 treatment, co-precipitation, coagulation, filtration, activated carbon, ozonation, and photochemical  
79 decolourization [12, 13]. These methods frequently share the inconvenience of incomplete  
80 degradation of the dye molecule, which leads to the formation of toxic by-products. These limits of  
81 conventional water treatment methods can be overcome by the use of advanced oxidation processes,  
82 which has the ability to completely mineralize the dyes, including the opening of the aryl ring.  
83 Usually, advanced oxidation processes consist of procedures in which active hydroxyl radicals act  
84 as strong oxidants for degradation of polluting materials. Most of these processes are based on the  
85 high oxidation capacity of hydroxyl radicals (2.8 V). One of the most effective methods among the  
86 advanced oxidation route is the use of UV rays combined with oxidant such as titanium dioxide.  
87 Titanium dioxide ( $\text{TiO}_2$ ) is well recognized as a low cost and efficient catalyst for degradation of  
88 organic matters [14]. The application of titanium dioxide as heterogeneous photocatalyst is well  
89 established for the remediation of water and air purification [15, 16]. For instance, the  
90 photocatalytic degradation of azo dyes in aqueous solution is based on photo activation of  $\text{TiO}_2$   
91 with UV light, which leads to a sequence of reactions resulting in the production of oxidants. The so  
92 formed compounds (hydroxyl radicals) can easily react with organic compounds on the  $\text{TiO}_2$   
93 surface.[17] However, since titanium dioxide has a band gap of 3.2 eV, which can be activated only  
94 under UV-light irradiation, efforts have been made to discover methods providing the  
95 photoactivation of this photocatalyst under visible light. Doping of  $\text{TiO}_2$  represents a widely used  
96 approach for developing  $\text{TiO}_2$  based materials useful for environmental applications [18]. Different  
97 methods for the synthesis of carbon doped  $\text{TiO}_2$  particles have been proposed to improve the  
98 photocatalytic activity [16, 19]. Recently different research groups highlighted the efficiency of a  
99 visible-light-active  $\text{TiO}_2$  photocatalyst prepared through carbon doping using glucose as the carbon  
100 source towards organic compounds [20-22].  
101 RhB is largely used to prove the efficiency of catalysts in general and for  $\text{TiO}_2$  in particular,  
102 towards organic matter [23-27]. Nevertheless, as stated above due to the possibility of incomplete

103 degradation of the dye molecule, to some extent, would be useful to clarify the difference between  
104 decolourization and degradation. In fact, a decolourization processes does not necessarily  
105 correspond to a complete degradation of the dye [28]. Furthermore, the presence of different  
106 photocatalytic degradation processes, such as chromophore cleavage, opening-ring, N-de-  
107 ethylation, and mineralization have also to be taken into account [29, 30].

108 The aim of this investigation is the study of the photodegradation process of the dye, RhB, induced  
109 by a carbon doped visible light-active TiO<sub>2</sub> photocatalyst. Furthermore, an accurate investigation of  
110 the decolourization and the photocatalytic activity of carbon doped TiO<sub>2</sub> toward RhB was  
111 accomplished. The final goal is to provide new tools for the challenging removal of dyes from  
112 water.

113

## 114 **2. Materials and Methods**

115 **2.1. Materials.** Glucose, titanium isopropoxide (97%), ethanol absolute, potassium chloride, sodium  
116 carbonate and Rhodamine B (RhB) were purchased from Sigma-Aldrich.

117 **2.2. Carbon-Doped Titanium.** Carbon-doped TiO<sub>2</sub> (CDT) was synthesized following the method  
118 reported by Ren et al.[21]. TiO<sub>2</sub> particles were prepared by the hydrolysis of titanium isopropoxide  
119 in ethanol performed in the presence of potassium chloride. The sample was continuously stirred to  
120 produce a white precipitate, and the obtained suspension was aged for 24 hours. The suspension  
121 after filtration was overdried to yield amorphous TiO<sub>2</sub> particles. Carbon-doped TiO<sub>2</sub> was  
122 synthesized by supplying a glucose solution to amorphous TiO<sub>2</sub> powder (0.25 g of TiO<sub>2</sub> and 0.018 g  
123 of glucose). The suspension was treated at 160 °C for 12 h and washed several times with water and  
124 ethanol before use.

125 **2.3. Rhodamine photodegradation.** Photocatalytic degradation of RhB was carried out by using  
126 CDT activated under visible light irradiation. Photocatalysis were performed by placing the samples  
127 in a homemade reactor. The photocatalytic activity was activated with lamps providing visible light  
128 (6500 K). The photoemission spectrum of the fluorescence lamps provides visible light in the range

129 of 400–800 nm. The distance between the light source and the bottom of the solution was ~15 cm.  
130 10 mg of CDT were added to 10 mL of RhB solutions at different concentrations (6 - 60 mgL<sup>-1</sup>) and  
131 mechanically stirred. The temperature was kept constant at 25 °C. Samples were air-equilibrated  
132 and placed in the reactor and treated with visible light. Aliquots of the sample were withdrawn,  
133 diluted 1:10 with water, centrifuged at 10000 rpm for 10 minutes and analyzed. Changes in RhB  
134 concentrations due to water evaporation were taken into account and corrected. Experiments were  
135 performed in duplicate, and results were the mean values. The initial RhB concentration was  
136 obtained by means of a calibration curve performed at 25 °C.

137 **2.4. Spectroscopic characterization.** The RhB decolourization was determined  
138 spectrophotometrically by means of a double-beam thermostated spectrometer (Cary 100-Varian) in  
139 the 200–800 nm region. The decolourization extent was followed at 554 nm, and its decrease was  
140 determined as the difference between initial and final solution concentrations with appropriate  
141 corrections based on blanks. The percentage of RhB decolourization was calculated as normalized  
142 absorbance ( $C/C_0$ , where  $C_0$  is the initial concentration of RhB and  $C$  is the concentration of RhB at  
143 time  $t$ ). Fluorescence measurements were performed using a Varian Eclipse spectrofluorimeter in a  
144 1 cm quartz fluorescence cuvette, at 25 °C. The excitation and the emission slits width were 5 mm.  
145 The excitation wavelengths utilized for this study were 495, 510, 530 and 554 nm.

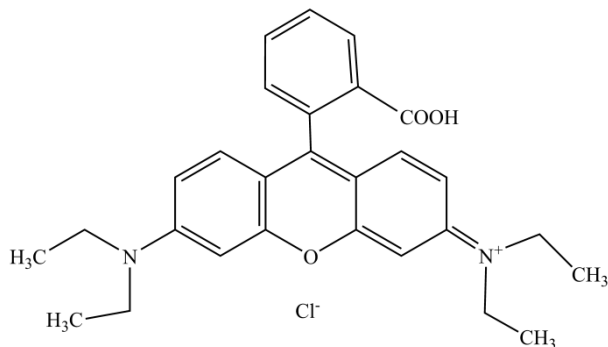
146 **2.5.  $\zeta$  potential.**  $\zeta$  potential measurements were performed by laser Doppler velocimetry using a  
147 Zetasizer-Nano ZS90 Malvern UK instrument operating with a 4 mW He–Ne laser (633 nm  
148 wavelength).

149 **2.6. Scanning electron microscopy (SEM).** Images were obtained with a Zeiss DSM 940  
150 instrument. Samples were deposited onto glass plates, left for 5 h at room temperature and sputtered  
151 with gold.

152

### 153 **3. Results and Discussion**

154 **3.1. RhB decolourization.** The photocatalytic activity of carbon-doped TiO<sub>2</sub> (CDT) was tested for  
155 the degradation of RhB (whose structure is reported in Fig.1) by lighting aqueous suspensions  
156 containing RhB and CDT particles with visible light radiations.

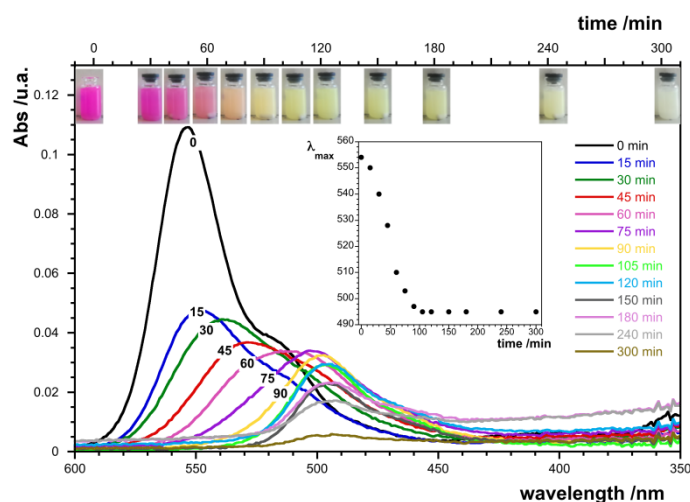


158 **Fig. 1.** Rhodamine B chemical structure.  
159

160 CDT is made of a mesoporous material obtained by the substitution of carbon atoms in the TiO<sub>2</sub>  
161 with values of the band gap energy, micropore size and surface area are 3.01 eV, 8 nm and 126.5m<sup>2</sup>  
162 g<sup>-1</sup> respectively [21]. SEM images, shows that freshly prepared CDT particles are monodisperse in  
163 agreement with the method introduced by Ren and coworkers (see SI1) [21]. A significant aspect of  
164 the whole photodegradation process is related to the surface charge of CDT particles [22]. Value of  
165  $\zeta$ -potential in aqueous solution was  $\sim 18$  mV (data not shown).

166 The first objective was an inspection on the decolourization ability of carbon doped TiO<sub>2</sub> towards  
167 RhB at fixed appropriate amounts of CDT particles and RhB. Fig. 2 shows the RhB adsorption  
168 spectra at different irradiation times. At a first sight it can be easily appreciated that: i) the  
169 characteristic absorption band of RhB at 554 rapidly decreases upon irradiation and completely  
170 disappears in about 60 min; ii) a progressive hypsochromic shift from 554 nm to 495 nm takes  
171 place. Fig. 2 also reports the pictures of the sample during the photoreaction at different time points.  
172 From a visual inspection of the sample it appears obvious that the characteristic brilliant pink color  
173 of RhB rapidly disappears, turning first into orange followed by yellow and white in agreement with  
174 the displayed spectra. Both blue shift and color variations suggest the existence of different  
175 intermediates produced in the presence of CDT under visible irradiation. Such intermediates share

176 an irradiation time dependent transient change of  $\lambda_{\max}$  starting from the initial RhB species at 554  
177 nm (inset of Fig. 2). From these results, it is evident that bleaching of the pink color (554 nm) does  
178 not correspond to the whole RhB degradation process. The maximum absorption shift from 554 to  
179 495 nm with the increased illumination time has been correlated in earlier studies performed in the  
180 presence of  $\text{TiO}_2$  and  $\text{O}_2$  with products coming from RhB N-de-ethylation [31].



181

182 **Fig. 2.** RhB UV-visible adsorption spectra and sample decolorization pictures as function of time exposure to visible  
183 light irradiation. Inset  $\lambda_{\max}$  shift.  $\text{Ti}/\text{RhB}$ : 150.  
184

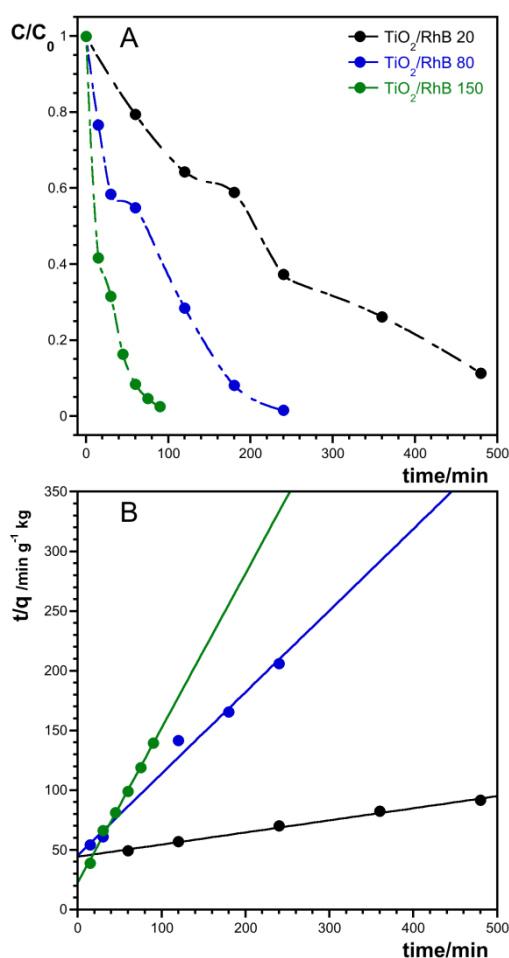
185 The effect of the amount of substrate on the decolorization process was tested by focusing only on  
186 changes in absorbance at 554 nm. From an applicative point of view it may be advantageous to  
187 combine both  $\text{TiO}_2$  and RhB in a unique parameter, namely the ratio between the catalysts particle  
188 (mg of  $\text{TiO}_2$ ) and the amount of dye (mg of RhB) [20].

189 Fig. 3A shows the decolorization ability of carbon doped titanium for samples with different  
190 values of the ratio  $\text{TiO}_2/\text{RhB}$  (20, 80 and 150) during exposure to visible light irradiation. The  
191 experimental data, expressed with normalized concentration ( $C/C_0$ ) of RhB as a function of time at  
192 25 °C, indicate that the RhB decolorization rate increases with increasing  $\text{TiO}_2/\text{RhB}$  ratios. The  
193 results are in agreement with a degradation process strictly related to the amounts of catalyst and



194 substrate, respectively as well as the ability of the substrate to be adsorbed on the surface of the  
 195 catalyst and other parameters such as pH and O<sub>2</sub> concentration [22, 31, 32].

196 As shown, the kinetics becomes slower with time, reaching the equilibrium after different time  
 197 intervals depending on the TiO<sub>2</sub>/RhB ratio. From the kinetics data, a dependence of the RhB  
 198 decolourization process on the TiO<sub>2</sub>/RhB ratio, typical of an adsorption process, was demonstrated,  
 199 foretelling a pivotal function of the adsorption event on the photoreaction in agreement with a  
 200 recent study performed on caffeic acid degradation in the presence of carbon doped TiO<sub>2</sub> [22].



201

202 **Fig. 3.** (A) RhB decolourization profiles as function of time. RhB under light irradiation with different amounts of  
 203 carbon doped TiO<sub>2</sub>. TiO<sub>2</sub>/RhB ratios 20, 80 and 150. (B) Fitting of the decolourization profiles to Eq. 1.

204

205 The decolourization profiles determined at different TiO<sub>2</sub>/RhB were fitted to a second-order kinetics  
 206 model by means of Eq. 1.

207

$$\frac{t}{q} = \frac{1}{k_2 q_e^2} + \frac{t}{q_e} \quad (1)$$

208 where  $k_2$  (kg/g per min) is the rate constant of second-order adsorption,  $q$  and  $q_e$  are the amounts of  
 209 RhB adsorbed on CDT at time  $t$  and at equilibrium, respectively (g/kg). The linear relationship, as  
 210 reported in Fig. 3B, indicates that a second-order kinetics is applicable. From Eq. 2 the half-life of  
 211 the process can be calculated as:

$$212 \quad t_{0.5} = \frac{1}{k_2 q_e} \quad (2)$$

213 The  $k_2$ ,  $q_e$  and  $t_{0.5}$  parameters at each TiO<sub>2</sub>/RhB ratio are presented in Table 1. From these data, it  
 214 emerges that the values of  $k_2$  increase with the increase of TiO<sub>2</sub>/RhB ratio (thus, with the decrease  
 215 of RhB concentration) while, the  $q_e$  values, as expected, decrease with increasing TiO<sub>2</sub>/RhB ratios.  
 216 The  $t_{0.5}$  values represent suitable parameters that underline the high decolourization rate attainable at  
 217 high values of TiO<sub>2</sub>/RhB ratios.

218 **Table 1.** Values of  $k_2$ ,  $q_e$ , and  $t_{0.5}$  at different TiO<sub>2</sub>/RhB ratio obtained by fitting the experimental data to Eqs. 1 and 2.  
 219

	$k_2$ (kg/g min)	$q_e$ (g/kg)	$t_{0.5}$ (min)
TiO <sub>2</sub> /RhB 20	2.31x10 <sup>-4</sup> (± 1.32x10 <sup>-5</sup> )	9.87 (± 0.46)	438 (± 32)
TiO <sub>2</sub> /RhB 80	0.01 (± 0.002)	1.46 (± 0.11)	68 (± 12)
TiO <sub>2</sub> /RhB 150	7.35 (± 0.93)	0.77 (± 0.03)	0.17(± 0.022)

220

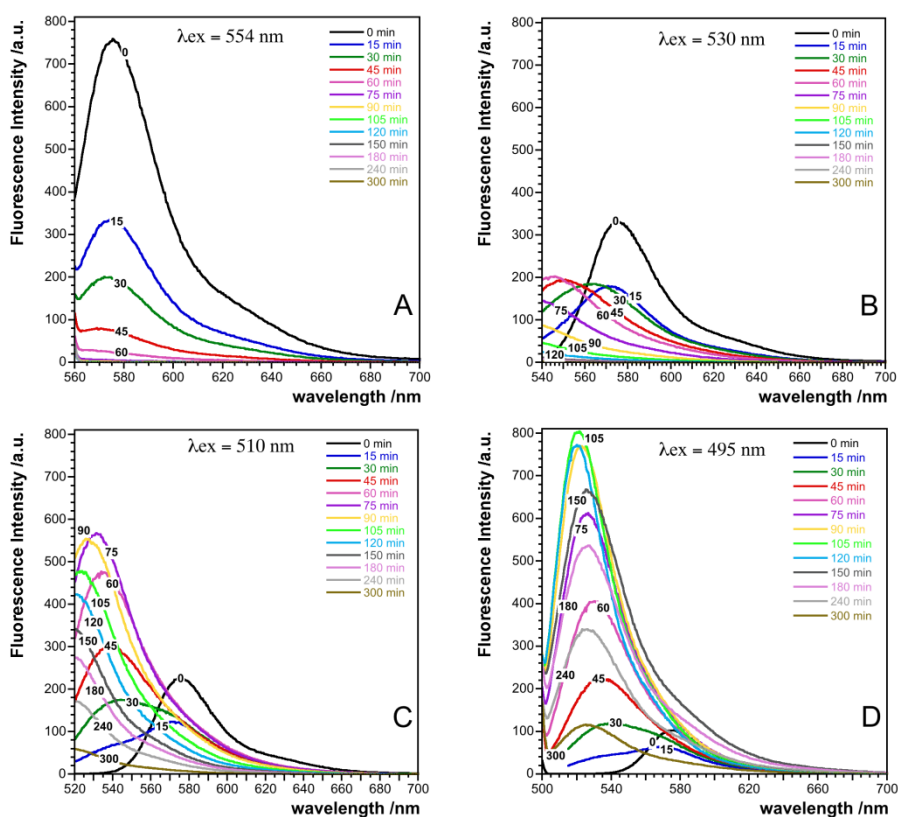
221 The low  $t_{0.5}$  value for the TiO<sub>2</sub>/RhB 150 should not surprise due to the large extent (excess) of the  
 222 adsorption particles in the earlier stages of the reaction [22].

223

### 224 **3.2 RhB degradation.**

225 So far, we showed that CDT particles activated by visible light can quickly decolorize RhB.  
 226 Furthermore, as inferred from Fig. 2, the presence of different peaks detectable during the  
 227 photodegradation process suggests the presence of different photoprocesses. To further investigate  
 228 this item we performed fluorescence measurements setting the excitation wavelength in  
 229 correspondence of some of the species identified through the adsorption maxima spectra of the UV-

230 Visible spectroscopy (see Fig. 2), namely at 554 nm, 530 nm, 510 nm and 495 nm. Fluorescence  
 231 spectroscopy has been shown to be a valuable procedure to monitor wastewater as well as an  
 232 investigating tool on biological macromolecules [33-37]. Fig. 4 shows fluorescence spectra during  
 233 the CDT mediated visible light RhB degradation carried out at the specified excitation wavelengths.  
 234 With this approach the identification of at least 4 different intermediates is ascertained. In fact, by  
 235 focusing one by one on the different excitation wavelength, the presence and the evolutions of  
 236 transient species is well deductible.



237

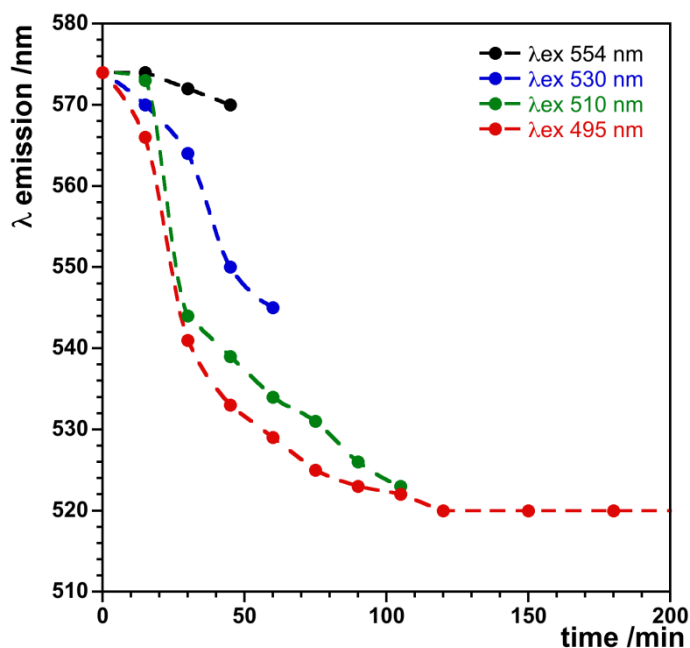
238 **Fig. 4.** RhB fluorescence spectra at different excitation wavelengths as function of visible light irradiation time. A:  $\lambda_{ex} = 554$  nm, B:  $\lambda_{ex} = 530$  nm; C:  $\lambda_{ex} = 510$  nm; D:  $\lambda_{ex} = 495$  nm. Ti/RhB: 150.

239

240

241 By exciting the RhB at 554 nm the only species that can be identified is the one that emits at 574  
 242 nm. This species completely disappears within 60 minutes of light exposure in the presence of CDT  
 243 (Fig. 4A). Exciting the Rhodamine at lower wavelengths revealed the existence of other degradation  
 244 intermediates. The excitation at 530 nm, indeed, allowed the detection of a first N-de-ethylation  
 245 product already after 30 minutes of light exposure, corresponding to the blue shifted emission  
 246 maximum. Some species, however, were not well identified because with the progress of the

247 reaction other intermediates emitting at even lower wavelengths were produced. As apparent in Fig.  
 248 4B, the spectra collected starting from the 75 min time point cropped and are better identified at  $\lambda_{ex}$   
 249 = 510 nm until the 90 min time point. This inconvenience is overcome by exciting the sample at  
 250 495 nm. In this condition, it is clear that after 105 minutes no more intermediates are formed and,  
 251 during the residual time, the degradation of the last intermediate occurs. Such results underline that  
 252 the whole photodegradation process does not end with the decolourization occurrence.  
 253 Furthermore by paying attention at the single emission peaks obtained with the different excitation  
 254 wavelengths both extents of intermediate lifetimes and the coexistence of intermediates can be  
 255 identified as a function of the irradiation times (Fig. 5). The main information of Fig. 5 other than  
 256 the emission wavelength shift is the fact that, after 15 minutes there are 3 or 4 different degradation  
 257 intermediates of RhB, other 4 species (at least) are detectable at 30 and 45 minutes. After 1 hour  
 258 there are 3 species and after 105 minute only one intermediate is detectable.



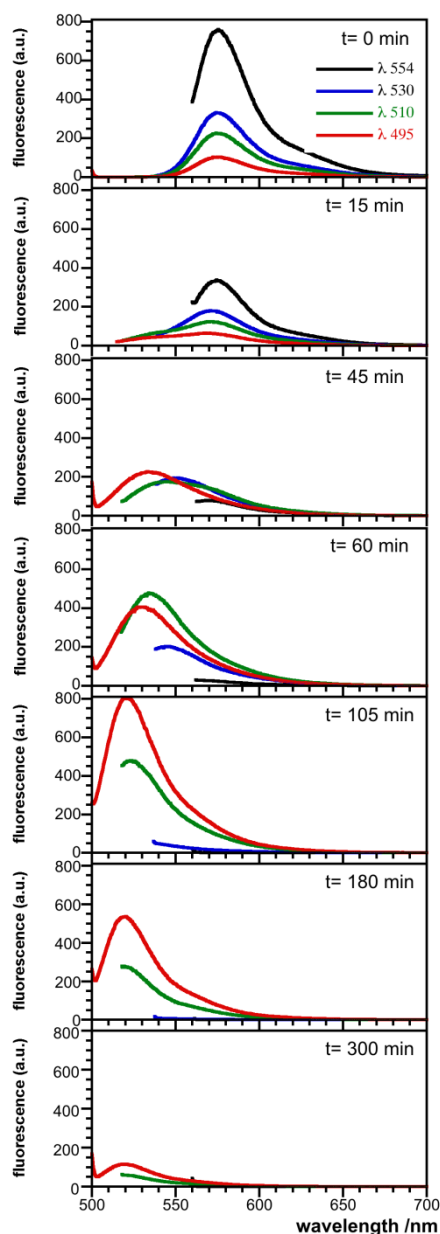
259

260 **Fig. 5.** RhB fluorescence. Emission wavelength shift according to the different excitation wavelength (554, 530, 510  
 261 and 495 nm) as function of irradiation time.

262

263 Evolutions of the combined fluorescence transient peaks at different reaction times reveal and  
 264 confirm that all the photoprocesses are connected each other (Fig. 6). In particular, by focusing on

265 the black and the red spectra of Fig. 6, referring to  $\lambda_{ex}$  of 554 and 495 nm, respectively, it is easy to  
266 identify the two main species, the first RhB that decomposes and the last intermediate that first  
267 increases in intensity, than decomposes, decreasing in emission intensity. The correlation between  
268 different fluorescence signals and intermediate evolutions is well highlighted. This evidence should  
269 be seen, therefore, as a very important step forward in demonstrating that fluorescence spectroscopy  
270 is a suitable tool concerning the subject-matter addressed.



271

272 **Fig 6.** Evolutions of the combined fluorescence transient peaks (554, 530, 510 495 nm) at different reaction times (0,  
273 15, 45, 60, 105, 180, 300 min).

274

275 Our results, based on the presence of different intermediates during RhB degradation in the  
276 presence of carbon-doped titanium dioxide are in agreement with literature data [29, 30, 38]. In  
277 these studies the evidence of such intermediates were identified by means of HPLC where it was  
278 reported that intermediates were produced one by one and every intermediates were transformed  
279 from the one just before itself.

280 Moreover, the role of both the catalyst and the dye properties is well established by the presence of  
281 two different photoprocesses, photobleaching and N-de-ethylation, that compete each other in the  
282 primary steps of the photoreaction [31]. Specifically, it has been shown that the formation of RhB<sup>+</sup>  
283 is a prerequisite for photobleaching, while •OH is responsible for the N-de-ethylation step.  
284 According to the oxidation potential of RhB and the band edges of TiO<sub>2</sub> the excited dye can inject  
285 electrons into the conduction band of TiO<sub>2</sub>, which become themselves cationic radicals and undergo  
286 further transformation to products [39]. The photosensitization reaction possibly includes the  
287 following reactions  $\text{RhB} + h\nu \rightarrow \text{RhB}^* + \text{TiO}_2 \rightarrow \text{RhB}^+ + \text{TiO}_2(e^-)$ .

288 Alternatively, in the presence of O<sub>2</sub> upon visible light irradiation, electrons can be excited directly  
289 into the TiO<sub>2</sub> conduction band and transferred to the adsorbed oxygen molecule to produce O<sub>2</sub><sup>-</sup> and  
290 then •OH with a strong oxidation power. Carbon doped titanium (CDT) used in this study is  
291 characterized by the substitution of carbon atoms in the TiO<sub>2</sub> photocatalyst that adds new states  
292 close to the valence band edge of TiO<sub>2</sub> (band gap energy of 3.01 eV) [20, 21]. Hereafter, the  
293 conduction band edge shifts to narrow the band gap. The arrangement of carbon into TiO<sub>2</sub> leads to  
294 the formation of carbonaceous species, which promotes light absorption in the presence of visible  
295 light [18, 32]. Meanwhile, the photogenerated hole oxidizes the adsorbed water molecule (OH<sup>-</sup>) to  
296 produce •OH radical. The adsorbed dye can thus react with •OH radical and be mineralized into  
297 CO<sub>2</sub> and H<sub>2</sub>O after a series of reactions [40]. Accordingly, it appears clear that to perform the whole  
298 RhB degradation all the criteria such as the presence of O<sub>2</sub> and visible light must met. Therefore  
299 with this study carbon doped titanium dioxide in the presence of visible light fulfils the condition to

300 avoid eventual competitive reaction that do not allow the whole RhB degradation process consisting  
301 in N-de-ethylation, chromophore cleavage, opening-ring, mineralization [29].

#### 302 **4. Conclusions**

303 The present study, centered on the removal of Rhodamine B from aqueous solutions, highlights the  
304 potential application of this technology for the elimination of dyes from wastewater, a fundamental  
305 goal in both the environmental and agronomical fields. Rhodamine B was degraded in the presence  
306 of carbon-doped TiO<sub>2</sub> through a photocatalytic process activated by visible light. Kinetics data  
307 obtained by means of UV–Vis spectroscopy revealed high degradation rate and substrate  
308 concentration dependence. The importance of adsorption process and visible light for such kind of  
309 catalyst is confirmed [22]. Fluorescence Spectroscopy allowed understanding that the degradation  
310 process of RhB was more than a simple adsorption based decolourization process, but passes  
311 through the formation of a series of intermediates generated from the N-de-ethylation reaction and  
312 gave information on the formation and co-existence of different intermediates. Such kind of  
313 evidence in agreement with previously study obtained by means of HPLC and LC-MS for  
314 Rhodamine B degraded in the presence of TiO<sub>2</sub>/SiO<sub>2</sub> the presence of Bi<sub>2</sub>WO<sub>6</sub> [28,29]. Furthermore,  
315 the synergic presence of carbon-doped titanium dioxide and visible light is an important condition  
316 to avoid the occurrence of competitive reactions that affect the whole RhB degradation process  
317 [29].

318

319

320

321

322

323

324

325 **Figure legends**

326 **Fig. 1.** Rhodamine B chemical structure.

327 **Fig. 2.** RhB UV-visible adsorption spectra and sample decolourization pictures as function of time  
328 exposure to visible light irradiation. Inset  $\lambda_{\text{max}}$  shift. Ti/RhB: 150.

329 **Fig. 3.** (A) RhB decolourization profiles as function of time. RhB under light irradiation with  
330 different amounts of carbon doped TiO<sub>2</sub>. TiO<sub>2</sub>/RhB ratios 20, 80 and 150. (B) Fitting of the  
331 decolourization profiles to Eq. 1.

332 **Fig. 4.** RhB fluorescence spectra at different excitation wavelengths as function of visible light  
333 irradiation time. A:  $\lambda_{\text{ex}} = 554$  nm, B:  $\lambda_{\text{ex}} = 530$  nm; C:  $\lambda_{\text{ex}} = 510$  nm; D:  $\lambda_{\text{ex}} = 495$  nm. Ti/RhB:  
334 150.

335 **Fig. 5.** RhB fluorescence. Emission wavelength shift according to the different excitation  
336 wavelength (554, 530, 510 and 495 nm) as function of irradiation time.

337 **Fig 6.** Evolutions of the combined fluorescence transient peaks (554, 530, 510 495 nm) at different  
338 reaction times (0, 15, 45, 60, 105, 180, 300 min).

339

340

341

342

343

344

345

346

347

348



350 **References**

- 351 [1] T. Robinson, G. McMullan, R. Marchant, P. Nigam, Remediation of dyes in textile effluent: A  
352 critical review on current treatment technologies with a proposed alternative, *Bioresour. Technol.*  
353 77 (2001) 247-255.
- 354 [2] G. Mishra, M. Tripathy, A critical review of the treatments for decolourization of textile  
355 effluent, *Colourage* 40 (1993) 35-38.
- 356 [3] A. Alinsafi, F. Evenou, E.M. Abdulkarim, M.N. Pons, O. Zahraa, A. Benhammou, A. Yaacoubi,  
357 A. Nejmeddine, Treatment of textile industry wastewater by supported photocatalysis, *Dyes Pigm.*  
358 74 (2007) 439-445.
- 359 [4] A. Bettoschi, A. Ceglie, F. Lopez, V. Meli, S. Murgia, M. Tamburro, C. Caltagirone, F. Cuomo,  
360 On the role of a coumarin derivative for sensing applications: Nucleotide identification using a  
361 micellar system, *J. Colloid Interface Sci.* 477 (2016) 8-15.
- 362 [5] F. Di Nezza, G. Guerra, C. Costagliola, L. Zeppa, L. Ambrosone, Thermodynamic properties  
363 and photodegradation kinetics of indocyanine green in aqueous solution, *Dyes Pigm.* 134 (2016)  
364 342-347.
- 365 [6] A. Cardone, F. Lopez, F. Affortunato, G. Busco, A.M. Hofer, R. Mallamaci, C. Martinelli, M.  
366 Colella, G.M. Farinola, An aryleneethynylene fluorophore for cell membrane staining, *Biochim.*  
367 *Biophys. Acta, Biomembr.* 1818 (2012) 2808-2817.
- 368 [7] F. Cuomo, F. Lopez, A. Ceglie, Templated globules - Applications and perspectives, *Adv.*  
369 *Colloid Interface Sci.* 205 (2014) 124-133.
- 370 [8] F. Cuomo, F. Lopez, M. Piludu, M.G. Miguel, B. Lindman, A. Ceglie, Release of small  
371 hydrophilic molecules from polyelectrolyte capsules: Effect of the wall thickness, *J. Colloid*  
372 *Interface Sci.* 447 (2015) 211-216.
- 373 [9] J. Rochat, P. Demenge, J.C. Rerat, Toxicologic study of a fluorescent tracer: rhodamine B,  
374 *Toxicol. Eur. Res.* 1 (1978) 23-26.
- 375 [10] R. Jain, M. Mathur, S. Sikarwar, A. Mittal, Removal of the hazardous dye rhodamine B  
376 through photocatalytic and adsorption treatments, *J. Environ. Manage.* 85 (2007) 956-964.
- 377 [11] B. Adinew, Textile effluent treatment and decolorization techniques - A review, *Chemistry* 21  
378 (2012) 434-456.
- 379 [12] J. Dasgupta, J. Sikder, S. Chakraborty, S. Curcio, E. Drioli, Remediation of textile effluents by  
380 membrane based treatment techniques: A state of the art review, *J. Environ. Manage.*, 147 (2015)  
381 55-72.

- 382 [13] V. Khandegar, A.K. Saroha, Electrocoagulation for the treatment of textile industry effluent -  
383 A review, *J. Environ. Manage.*, 128 (2013) 949-963.
- 384 [14] A. Fujishima, T.N. Rao, D.A. Tryk, Titanium dioxide photocatalysis, *J. Photochem. Photobiol.*  
385 *C 1* (2000) 1-21.
- 386 [15] H. Zhang, G. Chen, D.W. Bahnemann, Photoelectrocatalytic materials for environmental  
387 applications, *J. Mater. Chem.* 19 (2009) 5089-5121.
- 388 [16] B. Zhou, M. Schulz, H.Y. Lin, S.I. Shah, J. Qu, C.P. Huang, Photoelectrochemical generation of  
389 hydrogen over carbon-doped TiO<sub>2</sub> photoanode, *Appl. Catal. B.* 92 (2009) 41-49.
- 390 [17] I.K. Konstantinou, T.A. Albanis, TiO<sub>2</sub>-assisted photocatalytic degradation of azo dyes in  
391 aqueous solution: kinetic and mechanistic investigations - A review, *Appl. Catal. B* 49 (2004) 1-14.
- 392 [18] R. Dagher, P. Drogui, D. Robert, Modified TiO<sub>2</sub> For Environmental Photocatalytic  
393 Applications: A Review, *Ind. Eng. Chem. Res.* 52 (2013) 3581-3599.
- 394 [19] H. Irie, Y. Watanabe, K. Hashimoto, Carbon-doped anatase TiO<sub>2</sub> powders as a visible-light  
395 sensitive photocatalyst, *Chemistry Letters*, 32 (2003) 772-773.
- 396 [20] F. Cuomo, F. Venditti, G. Cinelli, A. Ceglie, F. Lopez, Olive mill wastewater (OMW) phenol  
397 compounds degradation by means of a visible light activated titanium dioxide-based photocatalyst,  
398 *Z. Phys. Chem.* 230 (2016) 1269-1280.
- 399 [21] W.J. Ren, Z.H. Ai, F.L. Jia, L.Z. Zhang, X.X. Fan, Z.G. Zou, Low temperature preparation and  
400 visible light photocatalytic activity of mesoporous carbon-doped crystalline TiO<sub>2</sub>, *Appl. Catal. B* 69  
401 (2007) 138-144.
- 402 [22] F. Venditti, F. Cuomo, A. Ceglie, P. Avino, M.V. Russo, F. Lopez, Visible Light Caffeic Acid  
403 Degradation by Carbon-Doped Titanium Dioxide, *Langmuir* 31 (2015) 3627-3634.
- 404 [23] T. Aarthi, G. Madras, Photocatalytic degradation of rhodamine dyes with nano-TiO<sub>2</sub>, *Ind. Eng.*  
405 *Chem. Res.* 46 (2007) 7-14.
- 406 [24] M. Hassanpour, H. Safardoust-Hojaghan, M. Salavati-Niasari, Degradation of methylene blue  
407 and Rhodamine B as water pollutants via green synthesized Co<sub>3</sub>O<sub>4</sub>/ZnO nanocomposite, *J. Mol.*  
408 *Liq.* 229 (2017) 293-299.
- 409 [25] W. Baran, A. Makowski, W. Wardas, The effect of UV radiation absorption of cationic and  
410 anionic dye solutions on their photocatalytic degradation in the presence TiO<sub>2</sub>, *Dyes Pigm.* 76  
411 (2008) 226-230.
- 412 [26] Y. Guo, J. Zhao, H. Zhang, S. Yang, J. Qi, Z. Wang, H. Xu, Use of rice husk-based porous  
413 carbon for adsorption of Rhodamine B from aqueous solutions, *Dyes Pigm.* 66 (2005) 123-128.
- 414 [27] D.S. Conceição, D.P. Ferreira, Y. Prostota, P.F. Santos, L.F. Vieira Ferreira, Photochemical  
415 behaviour of a new 1,2,3,4-tetrahydroxanthylum fluorescent dye with "rhodamine-like" structure in

416 liquid media and adsorbed onto a TiO<sub>2</sub> photo-responsive substrate, *Dyes Pigm.*, 128 (2016) 279-  
417 288.

418 [28] E. Adamek, W. Baran, J. Ziemiańska, A. Sobczak, The comparison of photocatalytic  
419 degradation and decolorization processes of dyeing effluents, *Int. J. Photoenergy* 2013 (2013).

420 [29] Z. He, C. Sun, S. Yang, Y. Ding, H. He, Z. Wang, Photocatalytic degradation of rhodamine B  
421 by Bi<sub>2</sub>WO<sub>6</sub> with electron accepting agent under microwave irradiation: Mechanism and pathway, *J.*  
422 *Hazard. Mat.* 162 (2009) 1477-1486.

423 [30] F. Chen, J. Zhao, H. Hidaka, Highly selective deethylation of Rhodamine B: Adsorption and  
424 photooxidation pathways of the dye on the TiO<sub>2</sub>/SiO<sub>2</sub> composite photocatalyst, *Int. J. Photoenergy*  
425 5 (2003) 209-217.

426 [31] P. Qu, J. Zhao, T. Shen, H. Hidaka, TiO<sub>2</sub>-assisted photodegradation of dyes: A study of two  
427 competitive primary processes in the degradation of RB in an aqueous TiO<sub>2</sub>-colloidal solution, *J.*  
428 *Mol. Catal. A: Chem.* 129 (1998) 257-268.

429 [32] C. Lettmann, K. Hildenbrand, H. Kisch, W. Macyk, W.F. Maier, Visible light  
430 photodegradation of 4-chlorophenol with a coke-containing titanium dioxide photocatalyst, *Appl.*  
431 *Catal. B* 32 (2001) 215-227.

432 [33] F. Lopez, F. Cuomo, P. Lo Nostro, A. Ceglie, Effects of solvent and alkaline earth metals on  
433 the heat-induced precipitation process of sodium caseinate, *Food Chem.* 136 (2013) 266-272.

434 [34] M.V. Russo, P. Avino, I. Notardonato, G. Cinelli, Cyanopropyl bonded-phase cartridges for  
435 trace enrichment of dioxins and chlorinated pesticides from water samples, *Chromatographia* 69  
436 (2009) 709–7017.

437 [35] M. Giustini, D. Angelone, M. Parente, D. Dini, F. Decker, A. Lanuti, A. Reale, T. Brown, A.  
438 Di Carlo, Emission spectra and transient photovoltage in dye-sensitized solar cells under stress  
439 tests, *J. Appl. Electrochem.* 43 (2013) 209-215.

440 [36] L. Travaglini, M. Gubitosi, M.C. Di Gregorio, N.V. Pavel, A. D'Annibale, M. Giustini, V.H.S.  
441 Tellini, J.V. Tato, M. Obiols-Rabasa, S. Bayati, L. Galantini, On the self-assembly of a tryptophan  
442 labeled deoxycholic acid, *Phys. Chem. Chem. Phys.* 16 (2014) 19492-19504.

443 [37] E.M. Carstea, J. Bridgeman, A. Baker, D.M. Reynolds, Fluorescence spectroscopy for  
444 wastewater monitoring: A review, *Water Research* 95 (2016) 205-219.

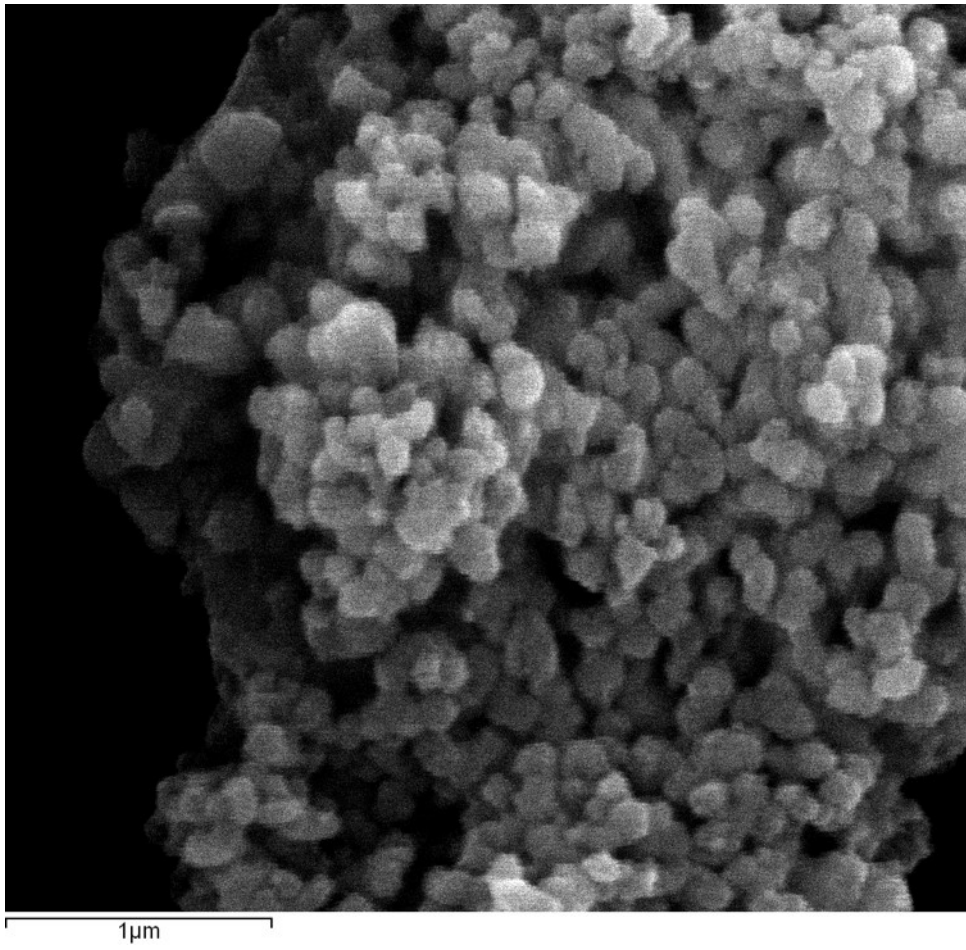
445 [38] C. Chen, W. Zhao, J. Li, J. Zhao, H. Hidaka, N. Serpone, Formation and identification of  
446 intermediates in the visible-light-assisted photodegradation of sulforhodamine-B dye in aqueous  
447 TiO<sub>2</sub> dispersion, *Environ. Sci. Technol.* 36 (2002) 3604-3611.

448 [39] M.R. Hoffmann, S.T. Martin, W. Choi, D.W. Bahnemann, Environmental Applications of  
449 Semiconductor Photocatalysis, *Chemical Reviews* 95 (1995) 69-96.

450 [40] V. Etacheri, C. Di Valentin, J. Schneider, D. Bahnemann, S.C. Pillai, Visible-light activation of  
451 TiO<sub>2</sub> photocatalysts: Advances in theory and experiments, J. Photochem. Photobiol. C 25 (2015) 1-  
452 29.

453

454



**SI1.** Freshly prepared Carbon doped titanium particles.